Journal of Microscopy, Vol. 169, Pt 3, March 1993, pp. 375–382.
Received 1 August 1992; accepted 4 January 1993

Measurement of co-localization of objects in dual-colour confocal images

E. M. M. MANDERS*, F. J. VERBEEK†‡ & J. A. ATEN*
**Laboratory for Radiobiology, University of Amsterdam, AMC, FO-212, Meibergdreef 9, 1105 AZ Amsterdam, The Netherlands*
†Department of Anatomy and Embryology, University of Amsterdam, AMC, K2-266, Meibergdreef 9, 1105 AZ Amsterdam, The Netherlands
‡Pattern Recognition Group, Delft University of Technology, PO Box 5046, 2600 GA Delft, The Netherlands

Key words. Co-localization, confocal microscopy, image analysis, image reconstruction, correlation, double labelling.

Summary

A method to measure the degree of co-localization of objects in confocal dual-colour images has been developed. This image analysis produced two coefficients that represent the fraction of co-localizing objects in each component of a dual-channel image. The generation of test objects with a Gaussian intensity distribution, at well-defined positions in both components of dual-channel images, allowed an accurate investigation of the reliability of the procedure. To do that, the co-localization coefficients were determined before degrading the image with background, cross-talk and Poisson noise. These synthesized sources of image deterioration represent sources of deterioration that must be dealt with in practical confocal imaging, namely dark current, non-specific binding and cross-reactivity of fluorescent probes, optical cross-talk and photon noise. The degraded images were restored by filtering and cross-talk correction. The co-localization coefficients of the restored images were not significantly different from those of the original undegraded images. Finally, we tested the procedure on images of real biological specimens. The results of these tests correspond with data found in the literature. We conclude that the co-localization coefficients can provide relevant quantitative information about the positional relation between biological objects or processes.

Introduction

Dual-colour confocal microscopy is based on the simultaneous or successive detection of two fluorochromes in the same specimen (Arndt-Jovin *et al.*, 1990; Carlsson, 1990; Mossberg & Ericsson, 1990). The data of the detected signals are stored in three-dimensional (3-D) dual-channel memory arrays (Dean *et al.*, 1990), a dual-colour image. One of the areas of special interest in dual-colour imaging is the frequency of coincidental objects—the degree of co-localization. For example, if the localization of the fluorochromes represents the distributions of different biochemical processes, it is of interest to analyse whether these processes take place at the same spot or are not correlated.

Due to the recent development of dual-colour confocal microscopy, co-localization studies of objects or processes in doubly labelled specimens have become feasible (Akner *et al.*, 1990; Draeger *et al.*, 1990; Kitamura *et al.*, 1990; Mossberg *et al.*, 1990; Sato *et al.*, 1990; Stamatoglou *et al.*, 1990; Fox *et al.*, 1991; Merdes *et al.*, 1991). Akner *et al.* (1991) presented a method to visualize the total overlap of two patterns by subtracting one component of an image from the other. This method provides a clear representation of complete overlap. A more quantitative method of measuring the degree of co-localization can be realized by using binary masks of both components of a dual-colour image (Lynch *et al.*, 1991). A method that does not use global intensity thresholding procedures is based on the use of Pearson's correlation coefficient (Manders *et al.*, 1992). By calculating the correlation between both grey values of the voxels, an indication of the amount of overlap can be obtained. However, the interpretation of this quantity is not unambiguous.

In this paper we introduce an alternative method, the calculation of two different quantities which are required to express the fraction of co-localizing objects in each component of a dual-colour image, named the co-localization coefficients. The method was tested on several synthesized images to obtain insight into the significance of the quantities of the co-localization

coefficients. The influence of image deterioration and image restoration on the result of the procedure was investigated. Finally, the method was tested on images of biological specimens to determine the utility of the procedure.

Theoretical background

Pearson's correlation coefficient is one of the standard procedures in pattern recognition (Gonzalez & Wintz, 1987) for matching one image with another and can be used to describe the degree of overlap between two patterns. It provides information about the similarity of shape without regard to the average intensity of the signals. Pearson's correlation coefficient (r_p) can be calculated from

$$r_p = \frac{\sum_i (R_i - R_{aver})\cdot(G_i - G_{aver})}{\sqrt{\left[\sum_i (R_i - R_{aver})^2 \cdot \sum_i (G_i - G_{aver})^2\right]}}, \quad (1)$$

where R_i and G_i are the grey values of voxel i of the red component and the green component of a dual-colour image, respectively. We called the two components of a dual-colour image the red component and the green component since Texas Red (or rhodamine) and FITC are often used in dual-colour confocal microscopy (Titus *et al.*, 1982; Mossberg & Ericsson, 1990). R_{aver} and G_{aver} are the average values of R_i and G_i, respectively. In Pearson's correlation the average grey values R_{aver} and G_{aver} are subtracted from the original grey values. Therefore, the value of this coefficient ranges from -1 to 1. The negative values of the correlation coefficient are difficult to interpret when the degree of overlap is the quantity to be measured.

When the average grey values of the voxels are not subtracted from the original grey values, a new coefficient can be defined as the overlap coefficient:

$$r = \frac{\sum_i R_i\cdot G_i}{\sqrt{\left[\sum_i (R_i)^2 \cdot \sum_i (G_i)^2\right]}} \quad (2)$$

The value of this coefficient ranges from 0 to 1. The product $(R_i\cdot G_i)$ in the numerator of the equation brings in a significant value only when R_i and G_i belong to a voxel of one of the co-localizing objects (with $R_i > 0$ and $G_i > 0$). Thus, the numerator is proportional to the number of co-localizing objects. In the same way, the denominator is proportional to the number of (co-localizing and not-co-localizing) objects in both components of an image.

A major advantage of the overlap coefficient is that it is not sensitive to differences in signal intensities between the components of an image caused by different labelling with fluorochromes, photo-bleaching or different setting of the amplifiers. This can be demonstrated by substitution of $R_i = a\cdot R_i'$ and $G_i = b\cdot G_i'$. This independence is a necessity for all overlap and co-localization measurements. A disadvantage of this method is that the result of the calculation is not unambiguous because of the strong influence of the ratio of the number of objects in both components.

To cancel out this effect the overlap coefficient r should be divided into two different coefficients by using for example

$$r^2 = k_1\cdot k_2, \quad (3)$$

with

$$k_1 = \frac{\sum_i R_i\cdot G_i}{\sum_i R_i^2} \quad (4)$$

and

$$k_2 = \frac{\sum_i R_i\cdot G_i}{\sum_i G_i^2} \quad (5)$$

Using these coefficients the degree of co-localization is expressed by two separate parameters. In these formulas k_1 and k_2 depend on the sum of the products of the red and the green intensities. Therefore, the coefficient k_1 is sensitive to differences in the intensity of the green signal (which can be demonstrated by substituting $G_i = b\cdot G_i'$). Analogously, k_2 depends linearly on the intensity of the red signal. Therefore, based on the split overlap coefficients (Eqs. 4 and 5), two other coefficients were defined that are not dependent on the intensities of the signals. These co-localization coefficients M_1 and M_2 are defined by

$$M_1 = \frac{\sum_i R_{i,coloc}}{\sum_i R_i}, \quad (6)$$

where $R_{i,coloc} = R_i$ if $G_i > 0$ and $R_{i,coloc} = 0$ if $G_i = 0$ and

$$M_2 = \frac{\sum_i G_{i,coloc}}{\sum_i G_i}, \quad (7)$$

where $G_{i,coloc} = G_i$ if $R_i > 0$ and $G_{i,coloc} = 0$ if $R_i = 0$. These coefficients, M_1 and M_2, are proportional to the amount of fluorescence of the co-localizing objects in each component of the image, relative to the total fluorescence in that component. M_1 and M_2, defined as the co-localization coefficients, can be determined even when the signal intensities in the two components differ strongly.

Material and methods

Applying the procedures presented in this paper, the

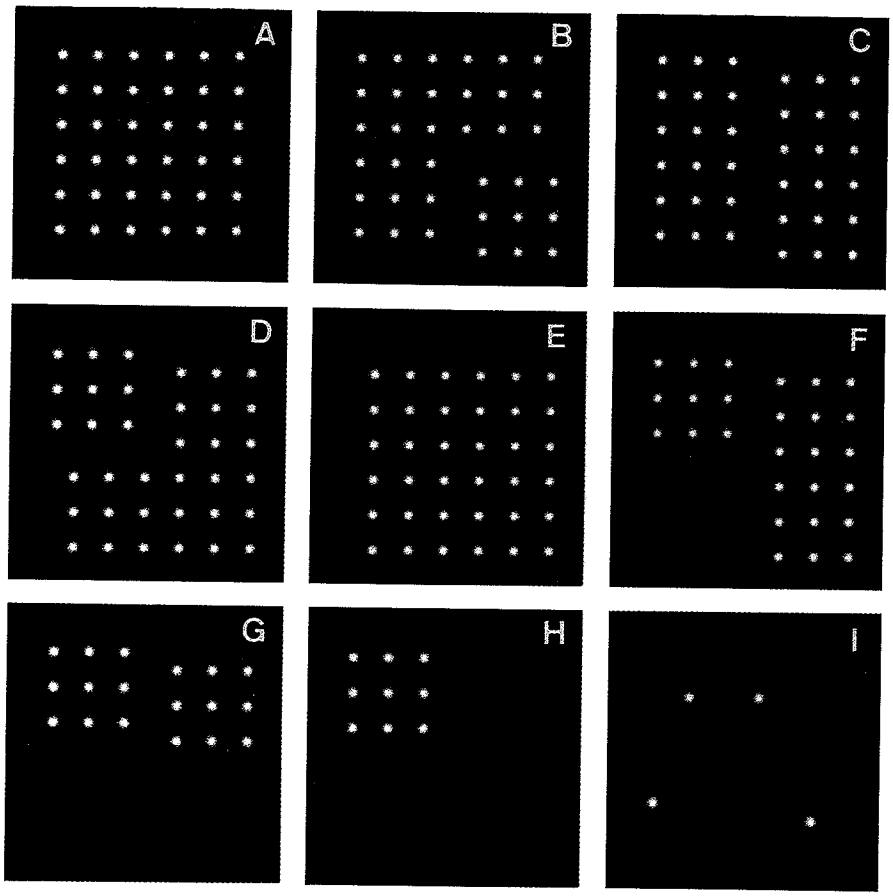

Fig. 1. Images containing test patterns of Gaussian objects. Simulated dual-colour images were obtained by combining image (A) with itself and with the other images, representing the components of a dual-colour image, e.g. a red and a green component. The degree of co-localization differs for each combination.

positional information of a 3-D image disappears because we are summing over all voxels of a 3-D image. This means that the result of the co-localization measurement algorithm applied to all data from a 3-D image is equivalent to the result of the algorithm applied to a representative part of the same 3-D data set (e.g. one optical section of a 3-D image). Therefore, it was acceptable to carry out all measurements on 2-D dual-colour test images (simulated optical sections). However, for testing the method on real biological specimens 3-D images were used in the calculations. For image processing and analysis the software package SCIL-IMAGE was used on a SUN Sparc workstation.

Test images

In our experiments we used several 2-D test images containing patterns of objects with Gaussian intensity distributions. The number of objects and the spatial distribution of the objects differed for each image. We constructed a Gaussian object with a diameter of 12 pixels full width at half maximum (FWHM). We then generated a 256 × 256 image with 36 objects at intervals of 32 pixels (Fig. 1A). Figure 1(E) was constructed by shifting all objects of Figure 1(A) 16 pixels to the right and 16 pixels down. All other test images (Fig. 1B–1D and 1F–1I) were constructed by copying parts of the images of Fig. 1(A) and (E). Simulated dual-colour images were obtained by combining two test images. The test images represented the parts of a dual-colour image, e.g. a red and a green component.

Measurement

To measure the degree of overlap and co-localization between the two components of a simulated dual-colour image, Pearson's correlation coefficient r_P, the overlap coefficient r and the co-localization coefficients M_1 and M_2 were used, as mentioned in the section on the theoretical background. The correlation, overlap and co-localization coefficients were tested on the synthesized images shown in Fig. 1.

Influence of background, noise and cross-talk

Images were degraded with background, cross-talk and Poisson noise to simulate the sources of deterioration that must be dealt with in practical confocal imaging, namely dark current, non-specific binding and cross-reactivity of fluorescent probes, optical cross-talk and photon noise.

Simulated background caused by 'dark current' of the photo multipliers was added to the original images using

$$R_{i,\mathrm{UBG}} = R_i + B_{\mathrm{DC}} \tag{8}$$

and

$$G_{i,\mathrm{UBG}} = G_i + B_{\mathrm{DC}}, \tag{9}$$

where B_{DC} is an integer value that represents the uniform background.

In addition to background caused by 'dark current', which is evenly distributed over the image, there is a further source of background in confocal images of biological subjects, namely background caused by non-specific binding of the fluorescent probes. Earlier experiments have shown that a typical intensity distribution of this type of background has high values at the central region of optical sections of biological specimens. This was simulated as follows:

$$R_{i,\mathrm{BG}} = R_i + B(r) \tag{10}$$

and

$$R_{i,\mathrm{BG}} = G_i + B(r), \tag{11}$$

with

$$B(r) = B_{X,Y} = B_{128,128}\cdot\left\{\sqrt{(2)} - \frac{\sqrt{[(x-128)^2 + (y-128)^2]}}{\sqrt{(2)}\cdot 128}\right\}, \tag{12}$$

which is an intensity distribution that has its maximum in the middle of the image and decreases linearly to zero at the borders of the image. The amount of background was expressed as the ratio of the average grey value of the added background and the maximum value of the signal.

To measure the influence of noise on the co-localization coefficients, noise was added to both components of the simulated dual-colour images. Because the major contribution to the noise in a confocal image was assumed to originate from quantum noise we used the Poisson distribution of probability:

$$P\{R_{i,\mathrm{noise}} = X\} = \mathrm{e}^{-R_i\cdot C}\cdot\frac{(R_i\cdot C)^{(X\cdot C)}}{(X\cdot C)!} \tag{13}$$

and

$$P\{G_{i,\mathrm{noise}} = X\} = \mathrm{e}^{-G_i\cdot C}\cdot\frac{(G_i\cdot C)^{(X\cdot C)}}{(X\cdot C)!} \tag{14}$$

to simulate an image with noise ($R_{i,\mathrm{noise}}$ and $G_{i,\mathrm{noise}}$). In these formulas P is the probability that the grey value of the new image equals X and the number of simulated photons per grey-value unit is represented in the multiplication factor C, which influences the signal-to-noise ratio (S/N).

The S/N was calculated using

$$(\mathrm{S/N})_{\mathrm{dB}} = 20\cdot\log\sqrt{\left[\frac{\sum_i (G_{i,\mathrm{noise}})^2}{\sum_i (G_{i,\mathrm{noise}} - G_i)^2}\right]}. \tag{15}$$

Cross-talk caused by cross-reactivity of the fluorescent probes (van den Engh *et al.*, 1985) and signal leak of the optical components (Carlsson & Mossberg, 1992) was simulated by using

$$R_{i,\mathrm{cross}} = (1-\alpha)\cdot R_i + \beta\cdot G_i \tag{16}$$

and

$$G_{i,\mathrm{cross}} = (1-\beta)\cdot G_i + \alpha\cdot R_i, \tag{17}$$

where α and β represent the cross-talk factors, and $R_{i,\mathrm{cross}}$ and $G_{i,\mathrm{cross}}$ the new grey values of the image with simulated cross-talk. For simplicity, we simulated equal cross-talk factors in both directions, i.e. $\alpha = \beta$.

Reconstruction

The reliability of co-localization measurement was investigated for several simulated dual-colour images. For this purpose first the coefficients of co-localization were calculated and the images were degraded with uniform and non-uniform background, cross-talk and noise. We first added 6% uniform and 4% non-uniform background and then simulated cross-talk with cross-talk factors α and β equal to 8%. Finally, we added photon noise with an S/N of 5 dB, which corresponds to 0·3 photons per grey-value unit. These values are representative of real confocal images. From these degraded images we tried to determine the coefficients of co-localization again.

Subsequently, the reliability of image reconstruction techniques was investigated. To do so, the degraded images were restored optimally, without taking into account the information on the input values used in the degrading procedure. Noise was reduced by filtering with a uniform 3×3 filter. Background was removed by applying a 31×31 uniform filter on each component of a dual-colour image, subtracting the result from the originals and setting the negative pixels to zero. Finally, 2-D intensity histograms of the dual-colour images were made. The angles of the distributions representing background pixels with the axes were measured. From these angles the cross-talk factors α and β were determined. Using the inverse of the transformation (Eqs. 16 and 17) that was used to simulate cross-talk, we corrected for cross-talk as optimally as possible.

The coefficients of co-localization were then calculated from these restored images. By comparing the results of these calculations with those of the undegraded images the reliability of the restoration procedure was assessed.

Table 1. Pearson's correlation (r_P), the overlap coefficient (r) and the co-localization coefficients (M_1 and M_2) performed on a set of generated dual-colour test images. These images were made by combining the image in Fig. 1(A) (red component) with the other images of Fig. 1 (green component). The co-localization coefficient clearly reflects the fraction of co-localizing objects in the red and green components of an image.

	Number of objects						
Figures	Red	Green	Co-localization	r_P	r	M_1	M_2
A A	36	36	36	1·00	1·00	1·00	1·00
A B	36	36	27	0·72	0·75	0·75	0·75
A C	36	36	18	0·44	0·50	0·50	0·50
A D	36	36	9	0·16	0·25	0·25	0·25
A E	36	36	0	−0·12	0·00	0·00	0·00
A F	36	27	9	0·22	0·29	0·25	0·33
A G	36	18	9	0·30	0·35	0·25	0·50
A H	36	9	9	0·48	0·50	0·25	1·00
A I	36	4	3	0·23	0·25	0·08	0·75

Application

To test the procedure on real biological specimens we used 3-D images of DNA replication patterns in doubly labelled nuclei of V79 Chinese hamster cells (Manders *et al.*, 1992). Cells were grown in three tissue culture flasks. At $T = 0$, iododeoxyuridine (IdUrd) was added to the medium of all cultures. At $T = 5$ min the IdUrd was washed away. DNA replicated during this 5-min period contains IdUrd. At $T = 0$, $T = 60$ min or $T = 180$ min chlorodeoxyuridine (CldUrd) was added to the medium of one of these three cultures. Five minutes after the addition of CldUrd the cultures were washed again. During the second pulse label, CldUrd was incorporated in replicating DNA. The cells were then fixed and spun down on slides. Applying an immunochemical staining procedure (Aten *et al.*, 1992), cells with the incorporated deoxyuridines (IdUrd and/or CldUrd) were stained with Texas Red and/or FITC, respectively. The fluorescence signals were recorded by CLSM in $2 \times 256 \times 256 \times 32$ data arrays. In this way two replication patterns originating from two different periods of the S-phase were visualized in the same cell. From each culture one cell was analysed. First, the coefficients M_1 and M_2 were calculated. Then, the images were reconstructed (noise reduction, background removal and cross-talk correction) and the coefficients were again calculated.

Results

Measurement

Table 1 shows the results of measurements of Pearson's correlation coefficient (r_P), the overlap coefficient (r) and the co-localization coefficients (M_1 and M_2). These measurements were performed using the combination of the image shown in Fig. 1(A) with itself and the other images of Fig. 1. Pearson's coefficient (Eq. 1) provides a value for the correlation between the intensity distributions of the components, but the overlap of the signals is better represented by the overlap coefficient r (Eq. 2). This is illustrated in the case of the combination of Fig. 1(A) and (E). Pearson's correlation coefficient is negative (Table 1: $r_P = -0{\cdot}12$), which indicates an inverse correlation of the signals. The fact that there are no overlapping objects in this example is expressed in a more perceptive way by the overlap coefficient r, which in this case has a value of 0·0. In the other cases shown in Table 1 with an equal number of objects in each component of an image, the overlap coefficient (r) exactly reflects the fraction of co-localizing objects in the images. When 18 objects out of 36 objects co-localize, the overlap coefficient (r) is equal to 0·5. However, when 9 out of 9 green objects colocalize with 9 of 36 red objects (the combination Fig. 1A/H), the overlap coefficient also equals 0·5. Consequently, the overlap coefficient provides useful information only when the number of objects in the red and green components are equal.

When the numbers of objects in the two components of the image are not equal, the co-localization coefficients M_1 and M_2 should be used. The co-localization coefficients M_1 and M_2 reflect the difference between the above-mentioned examples (Fig. 1A/C and 1A/H). This is illustrated by the values of the co-localization coefficients which were found to be 0·50 and 0·50 in the case of the combination of Figs. 1(A)/(C) and 0·25 and 1·00 in the case of the combination of Fig. 1(A)/(H), while the overlap coefficient r cannot

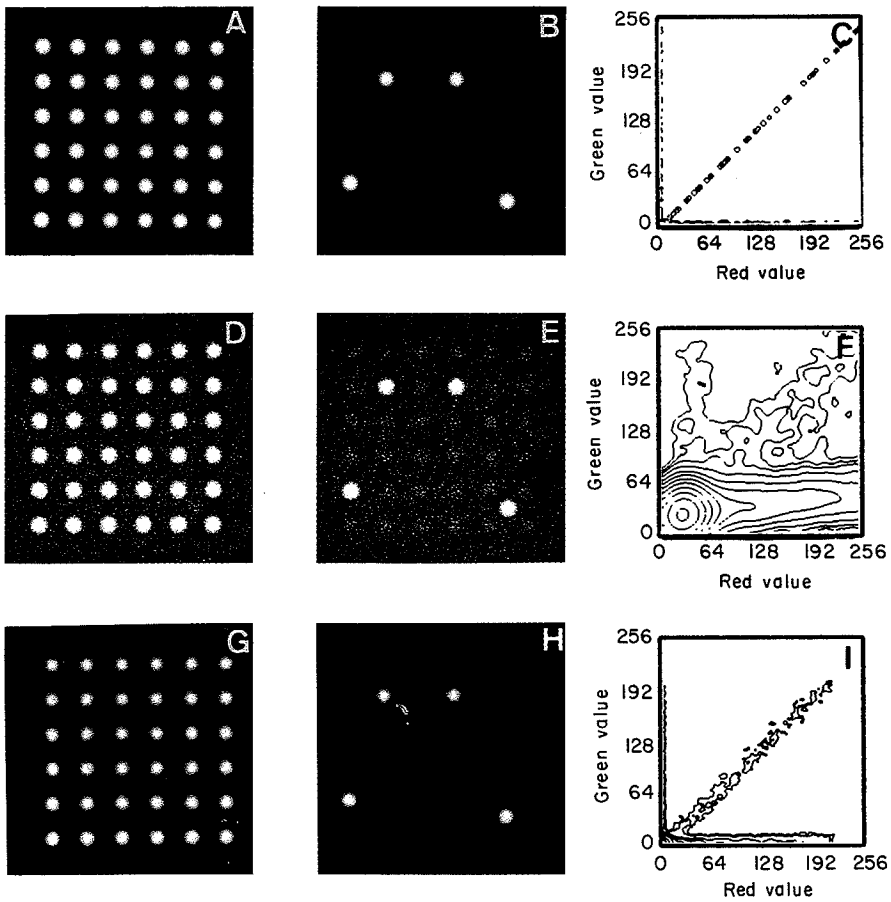

Fig. 2. The red (A, D and G) and green components (B, E and H), and the 2-D grey-value histograms (C, F and I) of a dual-colour image before image deterioration (A–C), after deterioration (D–F) and after image restoration (G–I). The co-localization coefficients M_1 and M_2 of the original image (A, B) equal 1/12 and 3/4, respectively. After degradation of the images with noise, background and cross-talk the values of the coefficients no longer reflect the amount of co-localization in the original image. Restoration of the degraded image resulted in a accurate determination of the coefficients M_1 and M_2, which were found to be equal to 0·09 and 0·77, respectively.

discriminate between these two cases and is equal to 0·50 (Table 1) in both cases. The interpretation is simple: one quarter of the red objects (Fig. 1A) co-localizes with green objects (Fig. 1H) and all green objects co-localize with red objects. Starting from the knowledge that the red component of the image contains 36 objects, it can be concluded that the green component contains only nine objects, which all co-localize with one of the red objects.

The co-localization coefficients are very sensitive for uniform and non-uniform background and cross-talk. When an image was deteriorated by one of these sources of degradation, the co-localization coefficients very rapidly converged to 1·0, as the number of non-zero voxels rapidly decreased. The coefficients were insensitive to Poisson noise as long as the S/N exceeded 10 dB. When the image was too noisy the coefficients diminished.

Reconstruction

We carried out an experiment to investigate the reliability of the image restoration procedures described above. We combined the images from Fig. 1(A) and (I) (which are shown again in Fig. 2A and B) and calculated the co-localization coefficients M_1 and M_2. The result $[M_1 = 0{\cdot}083\,(= 1/12)$ and $M_2 = 0{\cdot}75]$ implies that three of the four objects in Fig. 2(B) co-localize with objects in Fig. 2(A). Figure 2(C) shows the 2-D histogram of this dual-colour image. Near the axes the populations of pixels of the non-colocalizing objects are visible and the dots representing the pixels of co-localizing objects are located on the line $y = x$. After degrading the image with a 6% uniform and 4% non-uniform background, 8% cross-talk and 5 dB Poisson noise (Fig. 2D and E), the co-localization coefficients M_1 and M_2 were calculated again. The degradation of the signals is clearly visible in the bivariate histogram (Fig. 2F). The values of M_1 and M_2 both equal 1·0 and are not meaningful. After restoration of the image (Fig. 2G and H) the histogram (Fig. 2I) is very similar to that of the undegraded image. Finally, the values of M_1 and M_2 were found to be 0·09 and 0·77, respectively. When we depart from the knowledge that Fig. 2(G) contains 36 objects, then these results would imply that the image of Fig. 2(H) contains 4·2 objects of which 3·2 co-localize with objects of Fig. 2(G).

Application

The co-localization analysis procedure was tested on three

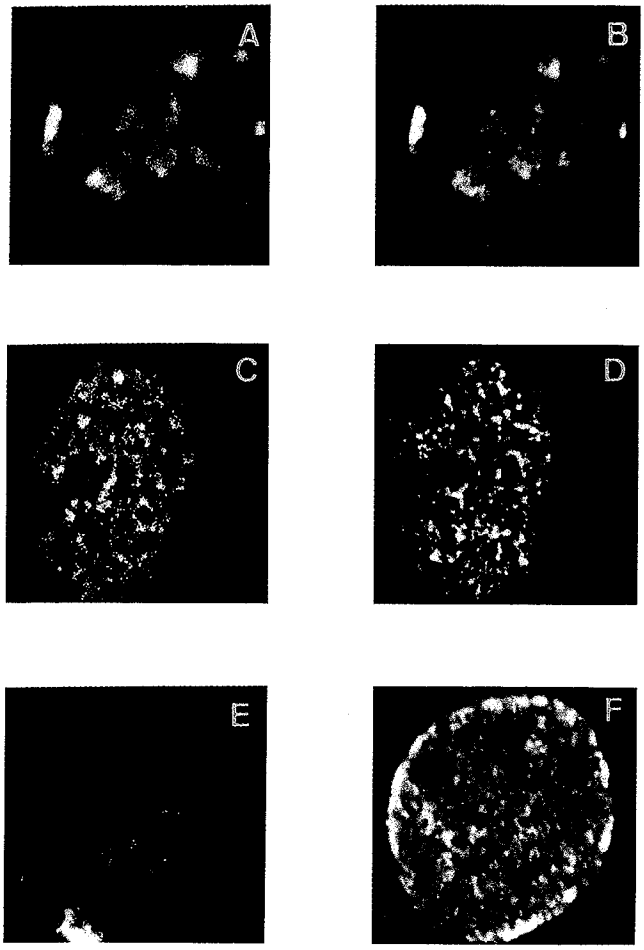

Fig. 3. The red (A, C and E) and green components (B, D and F) of optical sections of 3-D dual-colour confocal images of DNA replication patterns in three different cells. These cells were labelled with two different halogenated nucleotides (IdUrd and CldUrd) at the same time (A/B), with 1 h (C/D) and with 3 h (E/F) between the addition of the labels. Before image restoration the co-localization coefficients were all equal to 1·00. After restoration the co-localization coefficients M_1 and M_2 provide clear information about the amount of co-localizing objects in the components of an image. A/B: $M_1 = 0{\cdot}93$ and $M_2 = 0{\cdot}91$; C/D: $M_1 = 0{\cdot}27$ and $M_2 = 0{\cdot}28$; E/F: $M_1 = 0{\cdot}05$ and $M_2 = 0{\cdot}06$.

images of three different doubly labelled cells. Figure 3(A, B) show the red and the green components of the image of a cell that was labelled with both deoxyuridines at the same time (both at $T = 0$). The co-localization coefficients M_1 and M_2 of the original image both equal 1·0. After the reduction of background, cross-talk and noise, the coefficients equalled 0·93 and 0·91, respectively, which means that the images are almost identical. In Fig. 3(C) and (D) the components of a dual-colour image of a cell labelled at $T = 0$ (IdUrd) and $T = 60$ min (CldUrd) are shown. Again, the co-localization coefficients of the original image equalled 1·0, even though the image shows fewer co-localizing objects than the combination Fig. 5(A)/(B). After image restoration the co-localization coefficients showed that there were fewer co-localizing objects: $M_1 = 0{\cdot}27$ and $M_2 = 0{\cdot}28$. When the interval between the addition of each of the two labels was 3 h (Fig. 3E/F), very few overlapping objects could be identified ($M_1 = 0{\cdot}05$ and $M_2 = 0{\cdot}06$).

Discussion

To measure 3-D intensity distributions in dual-colour confocal images, the problem of a rigid data reduction must be dealt with. The reduction of a data set of four million image elements ($2 \times 256 \times 256 \times 32$) to one or two values implies a considerable loss of information. Therefore, it is important to define the information that should be derived from the images and to investigate to what extent the quality of the information is retained when it is expressed in terms of one or two variables. In this paper we have introduced a method to measure the co-localization of objects in dual-colour confocal images. The degree of co-localization has been defined as the ratio of the integral of the intensity distribution of co-localizing objects and the total intensity of the respective components of the image. We have investigated the quality of the results obtained with this method and determined its limitations.

Pearson's correlation coefficient has already proved to be a useful value for measuring the degree of overlap (Manders *et al.*, 1992). An accurate interpretaion of this coefficient, however, has not been given previously. Interpretation of the overlap coefficient as defined in this paper can be understood more easily. An image with an overlap coefficient equal to 0·5 implies that 50% of both components of the image overlap with the other part of the image. We must make one condition: the number of objects in both components of an image has to be more or less equal. When the number of objects is not equal, determination of the two co-localization coefficients M_1 and M_2 is the proper method. A number of possible applications can be mentioned. For example, specific organelles in a cell can be labelled and a specific process in this organelle can be detected with another label. Using this method, the fraction of organelles that carry out the process can then be calculated.

We have demonstrated that restoration of an image degraded with background, cross-talk and noise makes possible an accurate assessment of the values of the co-localization coefficients in the undegraded image. This provides confidence that the result of the calculations reflects the biological reality of the image. In addition, different intensities of the components of an image, caused by, for example, different amplifier settings, did not influence the values of the co-localization coefficients M_1 and M_2.

We have tested the method on images of cells doubly labelled with IdUrd and CldUrd at different periods of the S-phase. The results of the co-localization coefficients are in agreement with results of earlier studies (Manders *et al.*, 1992). The images of these replication patterns contain objects (labelled DNA) of quite different intensities, shapes and positions, in contrast with the objects in the synthesized images.

Acknowledgments

We thank C. Hersbach and C. Gravemeijer for the photography work, R. J. A. M. Baeten and J. Stap for experimental assistance and Dr A. C. Schoolwerth, Professor G. W. Barendsen, Professor J. Strackee and the anonymous referees for critical reading of the manuscript. This work has been partially sponsored by SPIN, project 3-D analysis and The European Communities, proposal No. 0104.

References

Akner, G., Mossberg, K., Wilkström, A., Sundqvist, K. & Gustafsson, J. (1991) Evidence for colocalization of glucocorticoid receptor with cytoplasmic microtubiles in human gingival fibroblasts, using two different monoclonal anti-gr antibodies, confocal microscopy and image analysis. *J. Steroid Biochem. Molec. Biol.* **39**, 419–432.

Akner, G., Sundqvist, K., Denis, M., Wilkström, A. & Gustafsson, J. (1990) Immunocytochemical localization of glucocorticoid receptor in human gingival fibroblasts and evidence for colocalization of glucocorticoid receptor with cytoplasmic microtubiles. *Eur. J. Cell Biol.* **53**, 390–401.

Arndt-Jovin, D.J., Robert-Nicoud, M. & Jovin, T.M. (1990) Probing DNA structures and function with multi-wavelength fluorescence confocal laser microscope. *J. Microsc.* **157**, 61–72.

Aten, J.A., Bakker, P.J.M., Stap, J., Boschman, G.A. & Veenhof, C.H.N. (1992) DNA double labeling with IdUrd and CldUrd for spatial and temporal analysis of cell proliferation and DNA replication. *Histochem. J.* **24**, 251–259

Carlsson, K. (1990) Scanning and detection techniques used in a confocal scanning laser microscope. *J. Microsc.* **157**, 21–27.

Carlsson, K. & Mossberg, K., (1992) Reduction of cross-talk between fluorescent labels in scanning laser microscopy. *J. Microsc.* **167**, 23–37.

Dean, P., Mascio, L., Ow, D., Sudar, D. & Mullikin, J. (1990) Proposed standard for image cytometry data files. *Cytometry*, **11**, 561–569.

Draeger, A., Amos, W.B., Ikebe, M. & Small, J.V. (1990) The cytoskeletal and contractile apparatus of smooth muscle: contraction bands and segmentation of the contractile elements. *J. Cell. Biol.* **111**, 2463–2473.

van den Engh, G.J., Trask, B.J. & Grey, J.W. (1985) The binding kinetics and interaction of DNA fluorochromes used in the analysis of nuclei and chromosomes by flow cytometry. *Histochemistry*, **84**, 501–508.

Fox, M.H., Arndt-Jovin, D.J., Jovin, T.M., Baumann, P.H. & Robert-Nicoud, M. (1991) Spatial and temporal distribution of DNA replication sites localized by immunofluorescence and confocal microscopy in mouse fibroblast. *J. Cell Sci.* **99**, 247–253.

Gonzalez, R.C. & Wintz, P. (1987) *Digital Image Processing*, 2nd edn., Addison Wesley Publication Company, Mass.

Kitamura, T., Gatmaitan, Z. & Arias, I.M. (1990) Serial quantitative image analysis and confocal microscopy of hepatic uptake, intracellular distribution and biliary secretion of a fluorescent bile acid analog in rat hepatocyte doublets. *Hepatology*, **12**, 1358–1364.

Lynch, R.M., Fogarty, K.E. & Fay, F.S. (1991) Modulation of hexokinase association with mitochondria analyzed with quantitative three-dimensional confocal microscopy. *J. Cell Biol.* **112**, 385–295.

Manders, E.M.M., Stap, J., Brakenhoff, G.J., van Driel, R. & Aten, J.A. (1992) Dynamics of three dimensional replication patterns during the S-phase, analyzed by double labelling of DNA and confocal microscopy. *J. Cell. Sci.* **103.3**, 857–862.

Merdes, A., Stelzer, E.H. & De Mey, J. (1991) The three-dimensional architecture of the mitotic spidle, analyzed by confocal flurorescence and electron microscopy. *J. Electron. Microsc. Tech.* **18**, 61–73.

Mossberg, K., Arvidsson, U. & Ulfjake, B. (1990) Computerized quantification of immunofluorescence labeled axon terminals and of co-localization of neurochemicals in axon terminals with a confocal scanning laser microscope. *J. Histochem. Cytochem.* **38**, 179–190.

Mossberg, K. & Ericsson, M., (1990) Detection of doubly stained fluorescent specimens using confocal microscopy. *J. Microsc.* **158**, 215–224.

Sato, M., Sardana, M.K., Grasser, W.A., Garsky, V.M., Murray, J.M. & Gould, R.J. (1990) Echistanin is a potent inhibitor of bone resorption in cultures. *J. Cell Biol.* **111**, 1713–1723.

Stamatoglou, S.C., Sullivan, K.H., Johansson, S., Barley, P.M., Burdett, I.D. & Hughes, R.C. (1990) Localisation of two fibronectin-binding glycoproteins in rat liver primary hepatocytes. Co-distribution *in vitro* of integrin (alpha 5 beta 1) and non-integrin (AGp110) receptors in cell–substratum adhesion sites. *J. Cell Sci.* **97**, 595–606.

Titus, J.A., Haugland, H., Sharrow, S.O. & Segal, D.M. (1982) Texas Red, a hydrophilic, red-emitting flurophore for use with fluorescein in dual parameter flow microfluorometric and fluorescence microscopy studies. *J. Immunol. Methods*, **50**, 193–204.